Inorganic Chemistry
Article
pubs.acs.org/IC

Indirect Magnetic Exchange between *o*-Iminosemiquinonate Ligands Controlled by Apical Substituent in Pentacoordinated Gallium(III) Complexes

Alexander V. Piskunov,*[†,‡] Irina V. Ershova,[†] Artem S. Bogomyakov,[§] Andrey G. Starikov,[⊥] Georgy K. Fukin,[†,‡] and Vladimir K. Cherkasov[†,‡]

[†]G. A. Razuvaev Institute of Organometallic Chemistry of Russian Academy of Sciences, Tropinina str. 49, Nizhny Novgorod 603950, Russian Federation

[‡]Nizhny Novgorod State University, Gagarina ave. 23, Nizhny Novgorod 603950, Russian Federation

[§]International Tomography Center, Siberian Branch of the Russian Academy of Sciences, 3a Institutskaya str., 630090 Novosibirsk, Russian Federation

[⊥]Southern Scientific Center of Russian Academy of Sciences, 41 Chehova Ave., 344006 Rostov on Don, Russian Federation

Supporting Information

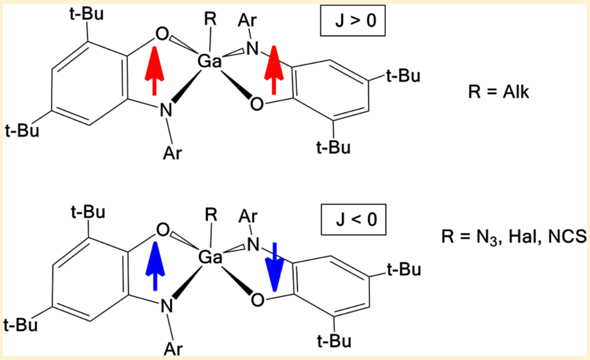

ABSTRACT: A number of pentacoordinated gallium complexes iSQ$_2$GaR (**1**−**7**) (R = Et (**1**), Me (**2**), N$_3$ (**3**), Cl (**4**), Br (**5**), I (**6**), NCS (**7**)) where iSQ is a radical anion of 4,6-di-*tert*-butyl-*N*-(2,6-diisopropylphenyl)-*o*-iminobenzoquinone were synthesized, and crystalline samples of **1**−**7** were characterized using magnetic susceptibility measurements. The character of magnetic exchange interaction between spins of *o*-iminosemiquinonate radicals was found to be strongly influenced by the nature of the apical substituent. The antiferromagnetic coupling is predominant when the apical position is occupied by halogens or other tested inorganic anions, and the value of exchange interaction parameter varies from −99 to −176 K for R = I and NCS, respectively. In the case of alkyl groups the ferromagnetic exchange prevails and, as the result, the triplet ground state for pentacoordianted biradical compounds was observed. Compounds **1**−**7** demonstrate a biradical X-band EPR spectrum in frozen toluene matrix. The molecular structures of **4**, **6**, and **7** have been established by single-crystal X-ray analysis. A computational DFT UB3LYP/6-31G(d,p) study was performed on complexes **1**−**7** in order to understand the reason for changes in the magnetic behavior of the related diradical gallium compounds. The calculations showed that the magnetic behavior of the complexes with inorganic anions is conditioned by the presence of antiferromagnetic exchange channel formed as a consequence of overlapping between donor atomic orbitals of iminoquinone with π-orbitals of halogen atoms (**4**−**6**) or nitrogen atom (**3**, **7**).

INTRODUCTION

The development of the approaches to creating new magnetic materials based on the high spin organic, organoelement, and coordination compounds is one of the topical problems of modern chemistry and material science. This trend is formed at the intersection of several fields of physics, chemistry, and material science. The creation of molecular magnets as the ultimate goal of this trend involves solving a number of smaller research objectives. One of them is a determination of the factors controlling the intramolecular magnetic exchange interactions between different spin centers in a molecule.

Metal complexes with stable radical ligands have been extensively investigated as potential building blocks for molecular magnet construction during past two decades.[1] An extensive array of information about metal complexes with paramagnetic radical anionic *o*-semiquinone and *o*-iminosemiquinone ligands is presented in the literature.[2] It seems to be useful to study such compounds with diamagnetic metal ions in order to construct magneto-structural correlations that in turn allow to observe clear magnetic interactions between organic radicals which are not complicated by the presence of the paramagnetic metal ion.[3] Using this approach, the authors[4] have found some correlation in the magnetic behavior of the biradical compounds of zinc. To date, there is a sufficiently wide data array about chemical and physicochemical properties of paramagnetic gallium derivatives which comprise the radical form of α-diimine type ligands.[5] Simultaneously, the investigation of the magnetic interactions between radical ligands in the coordination sphere of this metal was performed only for

Received: November 11, 2014
Published: June 8, 2015

DOI: 10.1021/acs.inorgchem.5b00520
Inorg. Chem. 2015, 54, 6090−6099

the single objects. For example, it was shown that the magnetic exchange interactions in the gallium tris-*o*-iminosemiquinonates are influenced by the dihedral angle between the planes of the radical ligands.[6] A similar conclusion can be reached by the analysis of the data obtained for the related hexacoordinated bis-*o*-iminosemiquinonato tin derivatives.[7] It was found that the character of the magnetic exchange between spins of organic radical ligands in the group 13 metal tris-*o*-semiquinonates depends strongly on the geometry of the coordination polyhedron of the complex.[8] The ferromagnetic exchange interactions dominate in the aluminum and gallium compounds with octahedral configuration, whereas the trigonal prismatic indium complexes demonstrate antiferromagnetic coupling.

The pentacoordinated metal complexes of the general formula iSQ_2MX (where iSQ − is a radical anion of different *o*-iminoquinones, X − halogen, alkyl, etc.) are well-known and extensively investigated in the case of transition metals.[9] The first example of such type complexes comprising iron(III) with two o-iminosemiquinonate (phenoxazin-1-onate) ligands and chlorine anion was published in 1994.[9a] Afterward the fine-tuning of the metal spin state in pentacoordinated bis-*o*-iminosemiquinonato Fe(III) complexes (iSQ_2FeX) was observed by K. Wieghardt and coworkers.[9b,c] The $S_t = {}^3/_2$ ground state was attained via intramolecular antiferromagnetic coupling between a high spin ferric ion ($S_{Fe} = {}^5/_2$) and two radical ligands whereas the $S_t = {}^1/_2$ form was generated from exchange coupling between an intermediate spin ferric ion ($S_{Fe} = {}^3/_2$) and two ligand radicals. The related cobalt(III) derivatives demonstrate singlet spin ground state with strong antiferromagnetic exchange between spins of organic radicals.[9d−g] Other pentacoordinated bis-*o*-iminosemiquinonate cobalt(III) derivatives containing an alkyl group bound to metal were found to be key intermediates in the Negishi-like cross-coupling of alkyl halides with organozinc reagents.[9h,i] The effective magnetic moment (2.77 μ_B at 300 K) for manganese(III) complex iSQ_2MnCl is caused by the strong antiferromagnetic coupling of two unpaired electrons of high spin metal ion d^4(S = 2) and two *o*-iminosemiquinonate paramagnetic ligands.[9g]

In our resent papers[10] we have observed that the magnetic behavior of two related indium(III) derivatives iSQ_2InX (where iSQ = 4,6-di-*tert*-butyl-*N*-(2,6-diisopropylphenyl)-*o*-iminobenzosemiquinone, X = Et[10a] and I[10b]) is quite different. In order to extend this study we have investigated a number of such derivatives of gallium(III). The present work is devoted to the variation of magnetic exchange interaction between radical ligands which is influenced by the apical substituent in the pentacoordinated bis-*o*-iminosemiquinonate gallium complexes with general formula iSQ_2GaR (where R = Et (**1**), Me (**2**), N_3 (**3**), Cl (**4**), Br (**5**), I (**6**), NCS (**7**)).

■ EXPERIMENTAL SECTION

General Remarks. All manipulations were carried out under vacuum using glass ampules. Solvents were purified using standard methods.[11] All reagents were purchased from Aldrich. The complexes **2**,[12] **4**−**6**,[13] and $EtGaI_2$[14] were synthesized according to the reported procedures. The IR spectra were recorded on a FSM-1201 spectrometer in a Nujol. The EPR spectra were obtained using a Bruker EMX spectrometer (9.75 GHz) and simulated with the WinEPR SimFonia Software (Bruker). The magnetic susceptibility of the polycrystalline complexes was measured with a Quantum Design MPMSXL SQUID magnetometer in the temperature range 2−300 K with magnetic field of up to 5 kOe. None of complexes exhibited any field dependence of molar magnetization at low temperatures. Diamagnetic corrections were made using the Pascal constants. The effective magnetic moment was calculated as $\mu_{eff}(T) = [(3k/N_A\mu_B^2)\chi T]^{1/2} \approx (8\chi T)^{1/2}$. The elemental analysis was performed on an elemental analyzer Euro EA 3000 instrument. The mass spectra of compounds were recorded on a mass spectrometer Polaris Q/Trace GC Ultra (Ion Trap analyzer), 70 eV, ion source temperature 250 °C, the sample temperature 50−450 °C.

Preparation of $imSQ_2GaEt$ (1). The solution of imSQNa[10b] (0.40 g, 1.055 mmol) in THF (25 mL) was added to the solution of $EtGaI_2$ (0.19 g, 0.528 mmol) in the same solvent (10 mL). The reaction mixture turned deep green. THF was removed under reduced pressure, and the residue was dissolved in hexane (25 mL). The reaction mixture was separated from the NaI precipitate by filtration. After slow evaporation of hexane solution, a green microcrystalline product of **1** was obtained. The total yield is 0.26 g (57%). Anal. Calcd for $C_{54}H_{79}GaN_2O_2$: C, 75.60; H, 9.28; Ga, 8.13%. Found: C, 75.89; H, 9.32; Ga, 8.10%. EI-MS: *m*/*z* 856 (100%), 857 (66.8%), 858 (95.2%), 859 (48.0%), 860 (19.3%) [M^+]. IR (Nujol, KBr) cm^{-1}: 1586 (s), 1438 (vs), 1355 (s), 1337 (s), 1320 (s), 1256 (s), 1219 (w), 1199 (m), 1171 (m), 1111 (m), 1101 (m), 1057 (w), 1042 (w), 1028 (m), 995 (m), 972 (w), 963 (w), 937 (w), 914 (m), 888 (m), 879 (m), 862 (m), 821 (w), 799 (s), 779 (w), 768 (m), 742 (w), 707 (w), 669 (w), 650 (w), 632 (w), 612 (w), 580 (w), 529 (m), 499 (w), 479 (w).

Preparation of $imSQ_2GaN_3$ (3). The solution of $imSQ_2GaI$ (**6**) (0.5 g, 0.528 mmol) in THF (25 mL) was added to 0.34 g of sodium azide (5.28 mmol). The reaction mixture was stirred at room temperature for 5 days. THF was removed under reduced pressure, and the residue was dissolved in hexane (25 mL). The reaction mixture was separated from the excess of NaN_3 and NaI precipitate by filtration. The following slow evaporation and storage of the hexane solution at −18 °C during a few hours led to the formation of crystalline green product **3**. The total yield is 0.20 g (43%). Anal. Calcd for $C_{52}H_{74}GaN_5O_2$: C, 71.71; H, 8.56; Ga, 8.01%. Found: C, 71.97; H, 8.58; Ga, 7.97%. EI-MS: *m*/*z* 869 (100%), 870 (50.1%), 871 (73.8%), 872 (34.3%), 873 (8.2%) [M^+]. IR (Nujol, KBr) cm^{-1}: 2095 (vs), 1585 (s), 1438 (vs), 1360 (s), 1337 (s), 1322 (s), 1297 (s), 1257 (s), 1221 (w), 1201 (m), 1174 (m), 1109 (m), 1058 (w), 1042 (w), 1028 (m), 995 (m), 975 (w), 935 (w), 917 (m), 892 (m), 881 (w), 863 (m), 823 (w), 800(s), 778 (w), 767 (m), 744 (w), 728 (w), 710 (w), 676 (w), 665 (w), 649 (w), 642 (w), 614 (w), 583 (w).

Preparation of $imSQ_2GaNCS$ (7)·0.5pentane. The solution of $imSQ_2GaI$ (**6**) (0.5 g, 0.528 mmol) in THF (25 mL) was added to 0.51 g of potassium thiocyanate (5.28 mmol). The reaction mixture was stirred at room temperature for a week. THF was removed under reduced pressure, and the residue was dissolved in hexane (25 mL). The reaction mixture was separated from the excess of KSCN and KI precipitate by filtration. The following slow evaporation of the pentane solution led to the formation of crystalline green product **7·0.5pentane**. The total yield is 0.25 g (53%). Anal. Calcd for $C_{55.5}H_{80}GaN_3O_2S$: C, 72.22; H, 8.74; Ga, 7.55; S, 3.47%. Found: C, 72.51; H, 8.77; Ga, 7.52; S, 3.45%. EI-MS: *m*/*z* 885 (100%), 886 (58.9%), 887 (82.1%), 888 (42.6%), 889 (12.4%) [M^+]. IR (Nujol, KBr) cm^{-1}: 2090 (vs), 1584 (s), 1432 (vs), 1392 (s), 1362 (s), 1333(s), 1255 (s), 1200(m), 1176 (m), 1106 (m), 1059 (w), 1044 (w), 1027 (m), 995 (m), 966 (w), 936 (m), 917 (s), 894 (m), 881 (m), 863 (m), 823 (m), 794 (s), 775 (w), 766 (s), 743 (w), 709 (w), 676 (m).

Single-Crystal X-ray Structure Determination of 4·hexane, 6·0.5hexane, and 7·0.5pentane. Crystals suitable for X-ray analysis were grown by the slow cooling of hexane and pentane solutions of **4**, **6**, and **7**, respectively. X-ray diffraction intensity data were collected at 100 K on Bruker D8 Quest (**4·hexane** and **6·0.5hexane**) and Agilent Xcalibur E (**7·0.5pentane**) diffractometers with graphite monochromated Mo Kα radiation (λ = 0.710 73 Å). The structures were solved by direct methods and were refined on F^2 using *APEX2*,[15] *SHELXTL*,[16] and *Crysalis Pro*[17] packages. All non-hydrogen atoms in **4·hexane**, **6·0.5hexane**, and **7·0.5pentane** were refined anisotropically. The hydrogen atoms in **4·hexane**, **6·0.5hexane**, and **7·0.5pentane** were placed in calculated positions and were refined in the riding model. *SADABS* (*APEX2 package*), *APEX2*,[15] and *ABSPACK* (*Crysalis Pro package*)[17] were used to perform area-detector scaling and

Table 1. Crystal Data and Structure Refinement of 4, 6, and 7

	$C_{58}H_{88}ClGaN_2O_2$ (**4·hexane**)	$C_{55}H_{81}GaIN_2O_2$ (**6·0.5hexane**)	$C_{55.5}H_{80}GaN_3O_2S$ (**7·0.5pentane**)
fw	950.47	998.83	923.01
cryst syst	monoclinic	monoclinic	monoclinic
space group	$P2_1/n$	$P2_1/n$	$P2_1$
unit cell dimensions			
a [Å]	16.1140(7)	20.0651(12)	12.60906(16)
b [Å]	20.3869(9)	21.6846(12)	22.9041(2)
c [Å]	17.0285(8)	25.8774(15)	18.84609(19)
β [deg]	91.3079(11)	106.4102(11)	90.0528(11)
V [Å^3]	5592.7(4)	10 800.7(11)	5442.74(10)
Z	4	8	4
density (calcd) [g/cm^3]	1.129	1.229	1.126
abs coeff [mm^{-1}]	0.580	1.120	0.584
F(000)	2056	4200	1988
cryst size [mm^3]	0.42 × 0.25 × 0.11	0.40 × 0.27 × 0.11	0.30 × 0.20 × 0.20
θ range for data collection [deg]	2.329–26.998	2.198–25.999	3.12–29.99
reflns collected	58 791	106 222	110 855
indep reflns	12 079 [R_{int} = 0.0389]	21 126 [R_{int} = 0.0367]	31 603 [R_{int} = 0.0523]
completeness to θ max	98.8%	99.4%	99.6%
data/restraints/params	12079/55/618	21126/93/1182	31603/2/1156
final R indices [$I > 2\sigma(I)$]	R1 = 0.0412	R1 = 0.0381	R1 = 0.0410
	wR2 = 0.1075	wR2 = 0.0983	wR2 = 0.0910
R indices (all data)	R1 = 0.0547	R1 = 0.0496	R1 = 0.0515
	wR2 = 0.1134	wR2 = 0.1036	wR2 = 0.0954
GOF on F^2	1.060	1.054	1.034
largest diff peak and hole [e/Å^3]	0.910/−0.624	1.999/−0.669	0.840/−0.610

absorption corrections. Crystal data and details of data collection and structure refinement for **4·hexane**, **6·0.5hexane**, and **7·0.5pentane** compounds are given in Table 1. CCDC-1051709 (**4·hexane**), -1051710 (**6·0.5hexane**), and -1009184 (**7·0.5pentane**) contain the supplementary crystallographic data for this paper. Copies of this information may be obtained free of charge from The Director, CCDC, 12, Union Road, Cambridge CB2 1EZ, U.K.; fax +44-1223-336033; e-mail deposit@ccdc.cam.ac.uk or http://www.ccdc.cam.ac.uk.

Computational Details. All density functional theory (DFT) calculations reported here were performed by means of the Gaussian 03 program package[18] with the hybrid B3LYP functional.[19] The standard 6-31G(d,p) basis was employed for all atoms with the exception of I, for which the full-electron basis dgdzvp was used. The stationary points on the potential energy surfaces (PES) were located by full geometry optimization with calculations of force constants and checked for the stabilities of Hartree–Fock solutions. The exchange coupling constants were calculated/evaluated by using broken symmetry technique[20a] according to the formula proposed by Yamaguchi.[20b,c]

■ RESULTS AND DISCUSSION

Syntheses. It has been previously shown that the reactions of *o*-amidophenolate gallium(III) complexes with different oxidative reagents lead to the formation of pentacoordinated diradical bis-*o*-iminobenzosemiquinolate metal derivatives. iSQ$_2$GaMe (**2**) was obtained as a result of oxidation of dimeric [APGaMe]$_2$ (AP = dianion of 4,6-di-*tert*-butyl-*N*-(2,6-diisopropylphenyl)-*o*-aminophenol) by dioxygen.[12] The halogen-containing derivatives iSQ$_2$GaHal (Hal = Cl(**4**), Br(**5**), I(**6**)) can be readily obtained as main products in the reaction of [AP$_2$Ga]GaI$_2$ with HgCl$_2$, HgBr$_2$, and I$_2$, respectively.[13] Another convenient way to compound **6** is an exchange reaction between iSQNa salt with GaI$_3$ (Scheme 1) in THF. It is necessary to note that this reaction is indifferent to the initial reagent stoichiometry.[13] The last product is a starting material for the preparation of complexes **3** and **7**. The prolonged stirring of THF solution of **6** with an excess of solid NaN$_3$ or KCNS gives **3** and **7**, respectively (Scheme 1).

There is a very intense characteristic single band $\nu(N_3)$ at 2095 cm^{-1} in the IR spectrum of **3**. The IR spectrum of **7** displays the ν(NCS) at 2088 cm^{-1} which is typical for N-coordinated thiocyanato ligands.[21]

EI-MS has been proven to be a very useful analytical tool for characterizing all complexes, which show the molecule-ion peak (see Experimental Section and Supporting Information) for compounds **1**–**7**. The [M − R]$^+$ peak (*m*/*z* 827 (100%), 828 (63.2%), 829 (81.4%), 830 (39.8%), 831 (12.4%)) is also observed in all of the cases.

Molecular Structures of 4·hexane, 6·0.5hexane, and 7·0.5pentane. The molecular structures of compounds **4**, **6**, and **7** were determined by single-crystal X-ray diffraction (Figures 1–3). The selected bond distances and angles for **4**, **6**, and **7** are collected in Table 1. The crystal structures of **2** and **5** have been published previously.[12,13] The most salient features of these crystallographic works are the following observations. All five crystals consist of neutral pentacoordinate molecules with a GaN$_2$O$_2$R coordination polyhedron (R = Me in **2**, Cl in **4**, Br in **5**, I in **6**, and NCS in **7**). Two O,N-coordinated *o*-iminobenzosemiquinonate ligands lie in trans-position with respect to each other. There are two crystallographically unique molecules in the asymmetric units of crystals **2**, **5**, **6**, and **7**. The presence of two asymmetric chelated rings in pentacoordinated gallium(III) complexes assumes chirality of the metal center, and both isomers (A and B) are presented in the unit cells (Figure 3). The angles and bond lengths of both units are quite similar. The geometry of coordination polyhedra in **1**–**7** can be described as a distorted tetragonal pyramid or trigonal bipyramid. The N(1), N(2), O(1), and O(2) atoms form the tetragonal pyramid base while the R substituent occupies the

Table 2. Selected Bond Distances (Å) and Angles (deg) for Complexes 4, 6, and 7

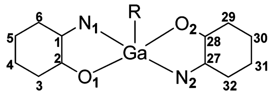

R = Cl (**4**), I (**6**), SCN (**7**)

	4	6	7
Ga(1)−O(1)	1.9611(12)	1.9650(16)	1.9655(13)
Ga(1)−N(2)	1.9651(14)	1.976(2)	1.9678(15)
Ga(1)−O(2)	1.9624(12)	1.9594(17)	1.9681(13)
Ga(1)−N(1)	1.9707(14)	1.967(2)	1.9723(16)
O(1)−C(2)	1.292(2)	1.287(3)	1.293(2)
O(2)−C(28)	1.294(2)	1.295(3)	1.295(2)
N(1)−C(1)	1.330(2)	1.331(3)	1.342(2)
N(2)−C(27)	1.334(2)	1.336(3)	1.334(2)
C(1)−C(6)	1.416(2)	1.412(3)	1.420(3)
C(1)−C(2)	1.450(2)	1.445(3)	1.457(3)
C(2)−C(3)	1.423(2)	1.431(3)	1.432(2)
C(3)−C(4)	1.376(2)	1.367(3)	1.376(3)
C(4)−C(5)	1.428(3)	1.433(4)	1.434(3)
C(5)−C(6)	1.361(2)	1.363(3)	1.362(3)
C(27)−C(32)	1.421(2)	1.412(3)	1.420(2)
C(27)−C(28)	1.445(2)	1.446(4)	1.461(3)
C(28)−C(29)	1.425(2)	1.426(3)	1.434(2)
C(29)−C(30)	1.370(3)	1.376(3)	1.376(3)
C(30)−C(31)	1.431(3)	1.431(4)	1.435(3)
C(31)−C(32)	1.353(2)	1.366(3)	1.372(2)
Ga(1)−R	2.1875(5)	2.5516(3)	1.9090(19)
R−Ga(1)−O(1)	98.83(4)	100.02(5)	97.20(7)
R−Ga(1)−N(2)	113.20(4)	113.50(6)	111.21(7)
O(1)−Ga(1)−N(2)	90.89(5)	90.52(8)	93.45(6)
R−Ga(1)−O(2)	99.39(4)	98.44(5)	96.56(7)
O(1)−Ga(1)−O(2)	161.78(6)	161.53(7)	166.22(6)
N(2)−Ga(1)−O(2)	82.05(5)	81.89(8)	82.34(6)
R−Ga(1)−N(1)	112.90(4)	114.11(6)	114.10(7)
O(1)−Ga(1)−N(1)	81.87(5)	81.75(8)	82.25(6)
N(2)−Ga(1)−N(1)	133.90(6)	132.39(9)	134.68(7)
O(2)−Ga(1)−N(1)	90.93(6)	90.95(8)	91.37(6)

Scheme 1. Syntheses of Complexes 1, 3, and 7

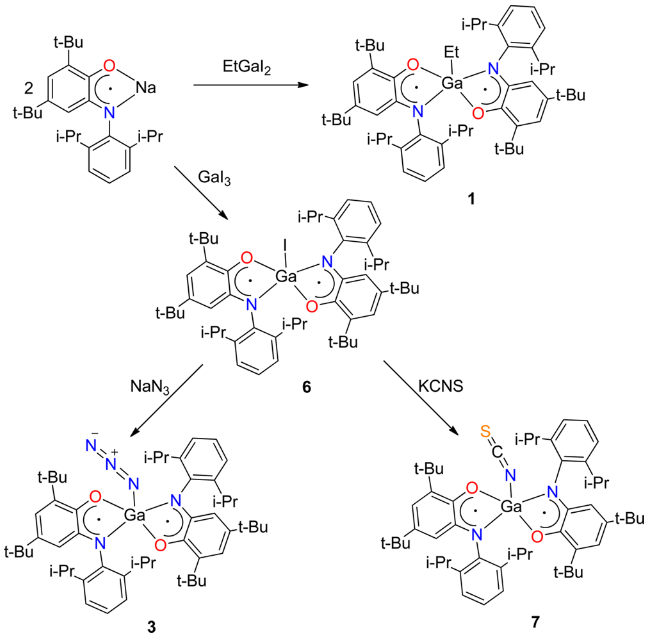

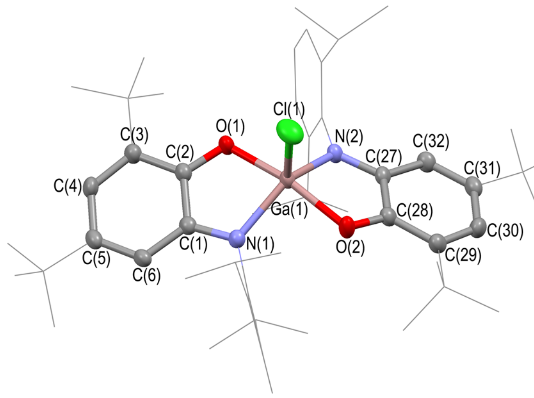

Figure 1. Molecular structure of **4**. Thermal ellipsoids are drawn at the 70% probability level. Hydrogen atoms are omitted.

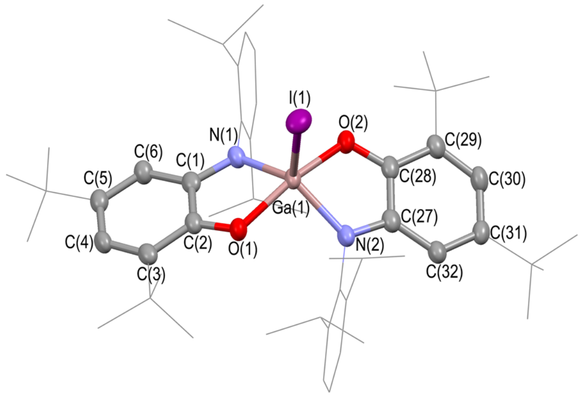

Figure 2. Molecular structure of **6**. Thermal ellipsoids are drawn at the 70% probability level. Hydrogen atoms are omitted.

apical site. The N(1), N(2), and R atoms lie in equatorial positions, and O(1), O(2) atoms are in apical sides in the case of the second polyhedron. The univocal choice of the coordination polyhedron type is unclear. The authors[22] propose to use the geometric parameter τ for the definition of coordination geometry in five-coordinate complexes. τ is equal to zero for a perfectly tetragonal geometry, while it becomes unity for a perfectly trigonal-bipyramidal geometry. All complexes under investigation have an intermediate value τ (average value for A and B isomers): 0.52, 0.47, 0.48, 0.48, 0.52 for **2**, **4**−**6**, and **7**, respectively. It is important to note that the geometrical details of the O,N-coordinated *o*-iminosemiquinolate ligands are identical in all five structures within 0.01 Å. The geometrical features of imSQ ligands in **2**, **4**−**6**, and **7** are typical for the radical anion form of such type of redox-active ligand and comparable with those in known *o*-iminobenzosemiquinonato metal complexes.[23] Thus, the C−O and C−N bond lengths have intermediate value between values characteristic for corresponding single and double bonds. The *o*-quinone alternation in six-membered C(1−6) and C(27−32) carbon rings is also observed. It appears in the separation of shorter C(3)−C(4) and C(5)−C(6) bonds by longer C(1)−C(2), C(2)−C(3), C(4)−C(5), and C(1)−C(6) bonds. We have performed the analysis of bond lengths for *o*-iminoquinone ligands in **2**, **4**−**6**, and **7** using utility of "metric oxidation state" (MOS) values for assessing bonding in catecholate and amidophenoxide ligands.[23] The MOS values obtained for structurally characterized complexes are consistent with the radical anion nature of the ligands and lie in the range from

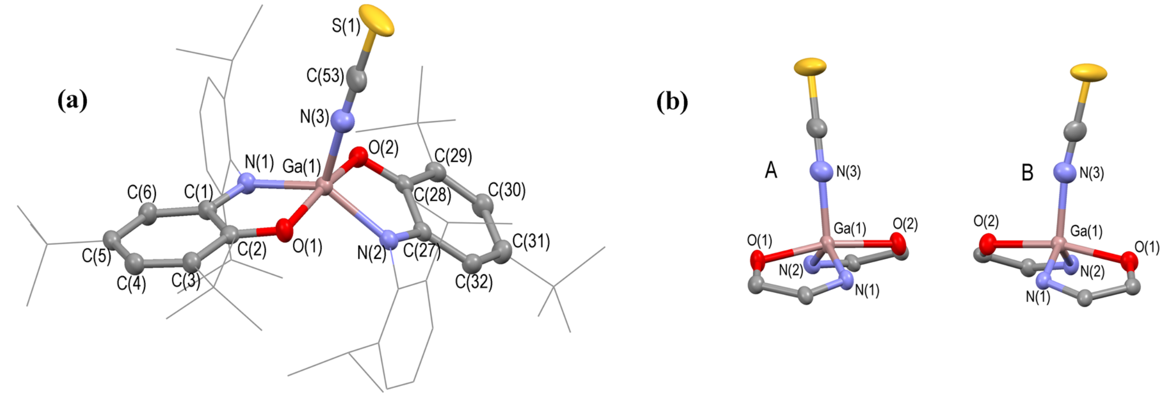

Figure 3. (a) Molecular structure of **7**. Thermal ellipsoids are drawn at the 70% probability level. Hydrogen atoms are omitted. (b) Fragments of structures of two independent units in crystal of **7** with 70% thermal probability ellipsoids.

−0.77(4) for **2** to −1.00(3) for **5**. Thus, the observed distribution of bond lengths in *o*-iminosemiquinonate ligands is in good agreement with the classical correlations and indicates the absence of additional π bonding between redox-active ligand and metal.

The Ga(1)−O(1) and Ga(1)−N(1) distances in **1**−**7** slightly exceed the sums of covalent radii of corresponding elements (1.88 Å for Ga−O and 1.93 Å for Ga−N).[24] It is typical for coordination of the radical anion form of the imQ ligand in previously reported metal complexes.[2] On the other hand, it should be noted that the difference in Ga−O(N) bond lengths was observed. These bonds are significantly longer in the alkyl derivative **2** (Ga−O 2.022 Å (av), Ga−N 2.000 Å (av)) than in the halide (**4**−**6**) or thiocyanate (**7**) derivatives (Ga−O 1.967 Å (av), Ga−N 1.974 Å (av)).

There are two important structural characteristics required for the discussion of the magnetic properties: the separation of radical centers and the dihedral angle formed by π radical systems. In conclusion it is necessary to note that these parameters are quite similar for all five structures **2**, **4**−**6**, and **7**. The average (for A and B isomers) radical separations estimated as distances between centroid (C(1)−C(2)) and centroid ((C27)−C(28)) are 5.00, 5.06, 5.06, 5.03, and 5.07 Å for **2**, **4**, **5**, **6**, and **7**, respectively. The average (for both isomers) dihedral angles between *o*-iminosemiquinone planes are 39.9°, 34.7°, 37.8°, 39.4°, and 40.3° for **2**, **4**, **5**, **6**, and **7**, respectively. Thus, the distortion between radical planes is almost the same for all complexes.

EPR Spectroscopy. Complexes **1**, **3**, and **7** (as well as **2**, **4**−**6** reported recently[12,13]) are paramagnetic both in solids and in solutions. The EPR spectra of polycrystalline samples of complexes **1**−**7** are quite similar at room temperature and 77 K. In all cases, only one resonance line was observed, with a g value of ca. 2.002, typical for a free radical. No hyperfine splitting could be seen. Peak to peak widths were of ca. 30 G, and no half-field resonance was detected. Toluene solutions of these compounds demonstrate a weak broad unresolved line at ambient temperature. Only in a frozen solvent matrix at 120 K will compounds give rise to EPR signals which clearly indicate the presence of the triplet species (Figure 4). The half-field EPR signals observed at $g = 4$ correspond to a forbidden transition ($\Delta m_s = 2$) (inset in Figure 4).

Although these signals are broadened, their hyperfine structure (quartet) can be distinguished. This hyperfine structure is caused by the presence of Ga atom (isotopes ^{69}Ga and ^{71}Ga possess nuclear spin $I = {}^3/_2$) in the molecules of **1**−**7**. Unfortunately, we were unable to determine precisely the zero-splitting parameters for complexes **1** and **5** since the diradical spectrum of the latter is too broad (Figure 5). The distance r between radical centers in molecules **2**−**4**, **6**, **7** can be estimated from zero field splitting parameters (Table 3) using dot dipoles approximation[25] ($r = (55\,600/2|D|)^{1/3}$). The calculated values r are very close to 5 Å for all complexes under investigation. It is necessary to note that this estimation is quite rough considering the delocalization of spin density through the *o*-iminosemiquinonate ligands. On the other hand, these values may be collated with X-ray data for compounds **2**, **4**−**7**. The obtained r (5 Å) corresponds well to the distance between bonds C(1)−C(6) and C(27)−C(28) centers (5.04, 5.06, 5.06, 5.03, and 5.07 Å for **2**−**4**, **6**, **7**, respectively) according to the X-ray data. These observations suggest that the EPR spectra recorded for triplet particles respond actually to biradical compounds **1**−**7**, and in general, these complexes retain their structure in solution.

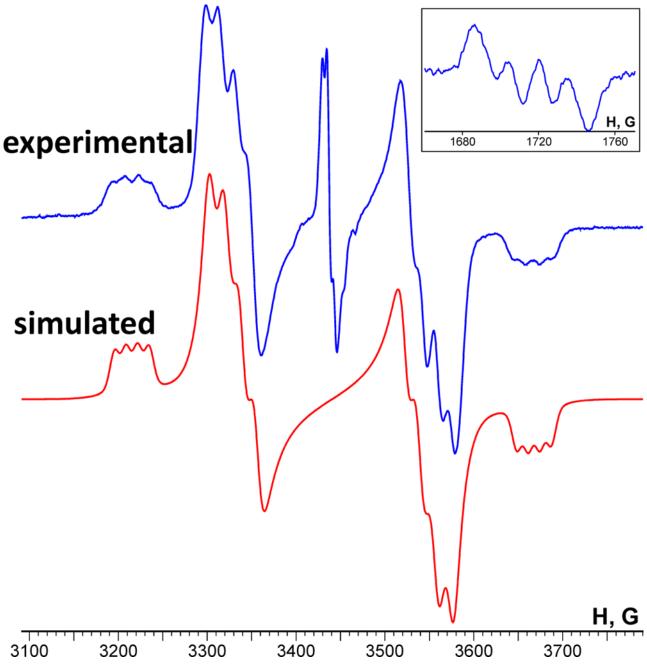

Figure 4. EPR spectra of **3** at $g = 2$ and $g = 4$ (inset) regions in toluene matrix at 120 K. Parameters are the following: $|D| = 633$ MHz, $|E| = 6$ MHz; $A_x = 48$ MHz, $A_z = 36$ MHz and $A = 45$ MHz for $g = 2$ and $g = 4$ signals, respectively.

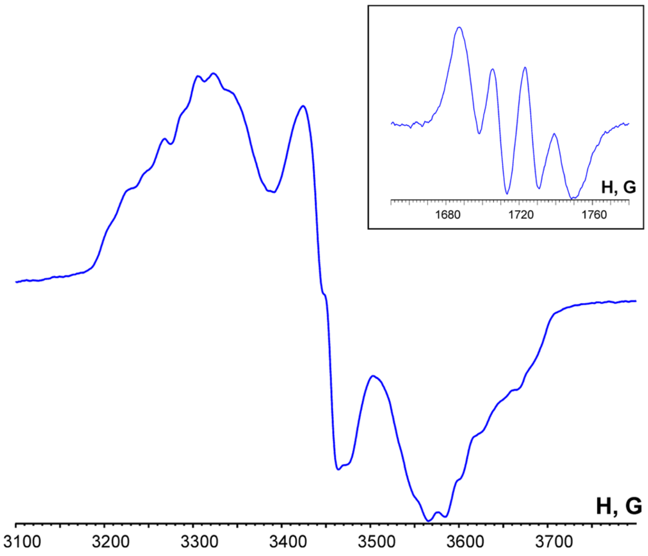

Figure 5. EPR spectra of **1** at $g = 2$ and $g = 4$ (inset) regions in toluene matrix at 120 K. Parameters are the following: $A = 49$ MHz for $g = 4$ signal.

Table 3. Zero Splitting Parameters of Complexes 2−7

	|D|, MHz	|E|, MHz
2	672	
3	633	6
4	622	
6	617	17
7	642	6

Magnetic Properties of Complexes 1−7. We used crystalline samples of complexes **2**, **4−7** in our magnetic susceptibility measurements. All of them contain one or one-half solvate molecule per biradical unit. We obtained compounds **1** and **3** as microcrystalline solids. They were dried under reduced pressure, and elemental analysis indicates the absence of any solvation in these samples.

The temperature dependences of the effective magnetic moments (μ_{eff}) are presented in Figure 6. The values of μ_{eff} at 300 K are close to the spin-only value ($\mu_{eff} = [(1.73)^2 + (1.73)^2]^{1/2} = 2.45\ \mu_B$), which is typical for system with two noninteracting paramagnetic centers with $S = {}^1/_2$ and $g = 2$, for all diradical complexes. However, the quite different temperature dependences were observed as a result.

For complexes with inorganic anions (**3−7**), μ_{eff} decreases with lowering temperature. This character of $\mu_{eff}(T)$ dependence is caused by a strong antiferromagnetic coupling between spins of *o*-iminosemiquinone ligands. At 2 K all samples nearly behave as diamagnetic species. Exchange coupled dimer model ($H = -2JS_1S_2$) describes experimental data adequately (Figure 6, solid lines). The best fit parameters (J, exchange interaction parameter; g-factor; monoradical impurity p) are the following: −105.2 ± 0.9 K (−72.6 cm^{-1}), 2.043 ± 0.009, 0 for **3**; −133.8 ± 0.5 K (−92.3 cm^{-1}), 2.011 ± 0.004, 0.0013 ± 0.0001 for **4·hexane**; −126.2 ± 0.8 K (−87.1 cm^{-1}), 2.004 ± 0.007, 0.0007 ± 0.0002 for **5·0.5Et$_2$O**; −99.5 ± 0.5 K (−68.6 cm^{-1}), 1.980 ± 0.005, 0.0059 ± 0.0004 for **6·0.5hexane**; and −176.4 ± 1.4 K (−121.7 cm^{-1}), 2.095 ± 0.012, 0 for **7·0.5pentane**.

Another magnetic behavior is observed for alkyl derivatives **1** and **2·0.5Et$_2$O**. The effective magnetic moments for these complexes change slightly with lowering temperature down to 50 K. Below 50 K the values of μ_{eff} increase gradually and then decrease slightly down to 5 K. Thus, in contrast to complexes **3−7**, the intramolecular exchange coupling between spins of two imSQ ligands in complexes **1** and **2·0.5Et$_2$O** is weaker and ferromagnetic in character. Decrease of μ_{eff} value near 5 K indicates the presence of weak intermolecular antiferromagnetic exchange coupling in solid samples of **1** and **2·0.5Et$_2$O**. Because the intra- and intermolecular values are small and comparable with each other, there is no appropriate model to estimate precisely magnetic exchange parameters.

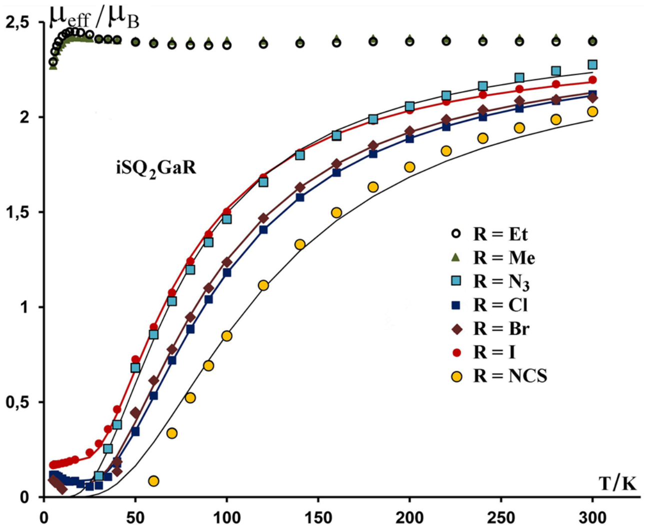

Figure 6. Temperature dependences of the effective magnetic moments of iSQ$_2$GaR type complexes: (black ○) **1**, (green ▲) **2·0.5Et$_2$O**, (light blue ■) **3**, (dark blue ■) **4·hexane**, (brown ◆) **5·0.5Et$_2$O**, (red ●) **6·0.5hexane**, (yellow ●) **7·0.5pentane**. Solid lines show the best fit curves (see text).

It is well-known that the solvation and resulting crystal package may have a significant impact on the magnetic properties of metal complexes.[26] The presence or absence of solvent molecules in the crystal cell does not change substantially the nature of the magnetic exchange in compounds under investigation. It becomes clear by the comparison of magnetic behavior of compounds **1** and **2·0.5Et$_2$O**.

Thus, the variation of the apical substituent can significantly change not only the value but also the sign of the exchange coupling energy between spins of *o*-iminosemiquinonate radical anions in pentacoordinated metal complexes. It is noteworthy that these changes take place even with the keeping of the complex geometry.

To the best of our knowledge, the few examples of the fine control of the magnetic exchange between magnetic centers in related *o*-semiquinonate copper(II) complexes by nonradical auxiliary ligands were described to date.[27a] Another striking case was a family of dinuclear cobalt complexes with bridging bis(dioxolene) ligands derived from 3,3,3′,3′-tetramethyl-1,1′-spirobis(indane-5,5′,6,6′-tetrol) and ancillary ligands based on tris(2-pyridylmethyl)amine. Methylation of the ancillary ligand influences the redox state of the complex, governing the distribution of electrons between the cobalt centers and the bridging ligands.[27b]

DFT Calculations. In order to determine the cause of the variation of magnetic behavior of bis-*o*-iminosemiquinonate gallium compounds, the quantum chemical calculations for complexes of the type iSQ$_2$GaR have been performed.

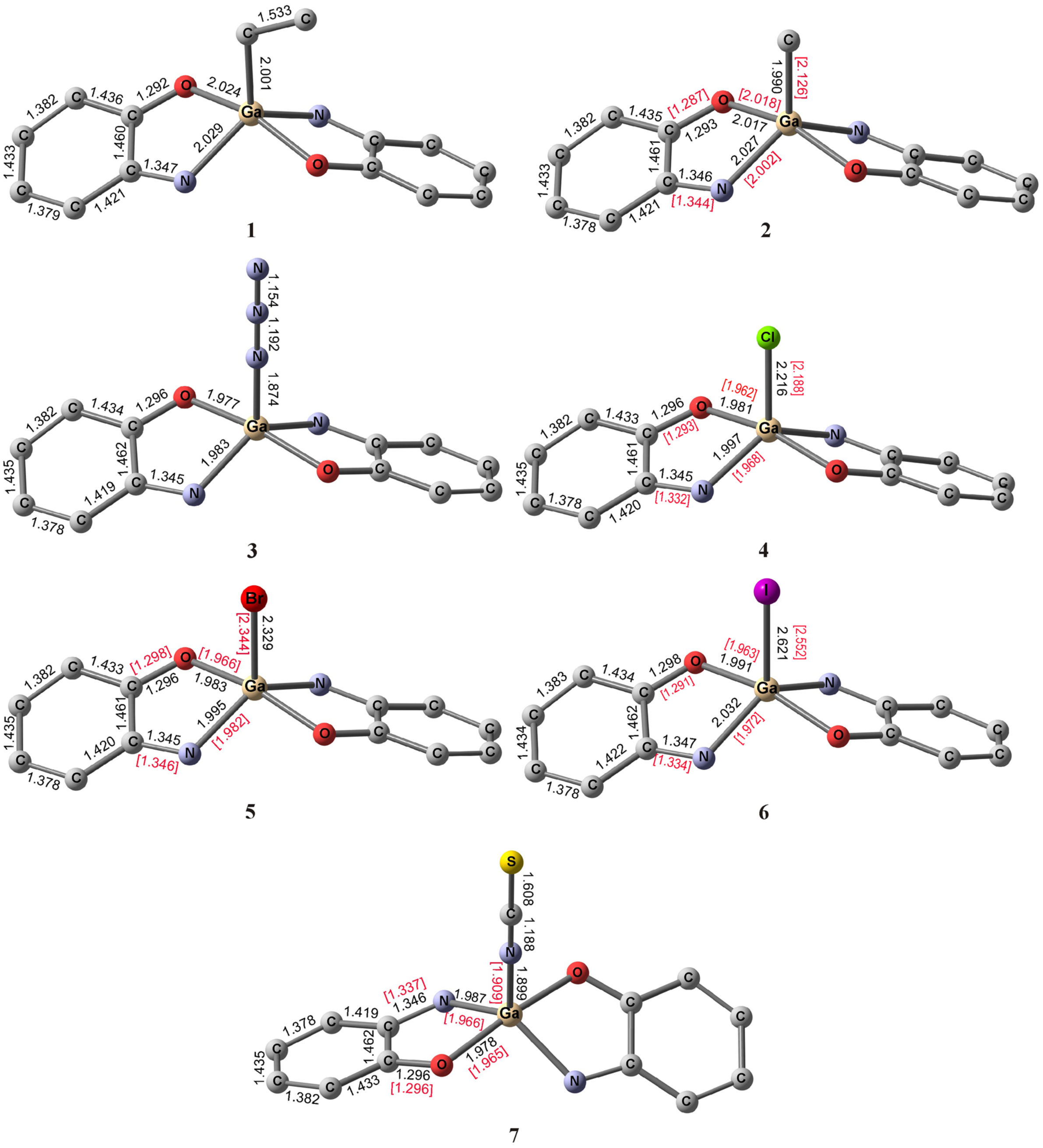

Figure 7. Optimized geometries of complexes **1**−**7**, calculated by the DFT UB3LYP/6-31G(d,p) method. Red figures given in brackets are average experimental values.[12,13] Hydrogen atoms and alkyl and phenyl groups are omitted for clarity. The bond lengths are given in angstroms (Å).

According to the calculations, the optimized geometries of complexes **1**−**7** on the triplet PES are in good agreement with the X-ray data (Figure 7). The constants *J* estimated using the BS-technique reproduce well the character of the exchange interactions (Table 4). The magnetic behaviors of complexes **1** and **2** containing alkyl groups are characterized by weak ferromagnetic coupling that is in agreement with the experimental data, while the unpaired electrons are antiferromagnetically coupled in compounds **3**−**7** with inorganic anions.

It was established earlier that the antiferromagnetic exchange interactions between spins of paramagnetic centers were observed in bis-chelates of the transition metals (Ni, Cu) containing two iminoquinone (phenoxazin-1-one) ligands,[9a,28a] while the exchange coupling is ferromagnetic in character in the

Table 4. Theoretical (J_{theor}) and Experimental (J_{exp}) Exchange Coupling Constants of Complexes 1−7, Calculated by the DFT UB3LYP/6-31G(d,p) Method

	J_{theor}, cm^{-1}	J_{exp}, cm^{-1}
1	45	-
2	45	-
3	−91	−72.6
4	−85	−92.3
5	−48	−87.1
6	−44	−68.6
7	−62	−121.7
7_{exp}	−122	

isostructural zinc compound.[28b] Analogous results were obtained for transition metal complexes with semiquinone ligands. The exchange interactions in such types of compounds have been shown to be antiferromagnetic and not depend on stereochemistry of the complexes.[29] The exchange coupling is determined by the superexchange channel, in which singly occupied molecular orbitals (SOMOs) of semiquinonate radicals and d-orbitals of metal atom are involved.[27,30] At the same time, complexes of semiquinones with non-transition-metals display ferromagnetic exchange interactions. Thus, Al(III) and Ga(III) compounds with three quinone ligands demonstrate ferromagnetic coupling between unpaired electrons of radical-containing ligands.[8a−c] The exchange character in such compounds was qualitatively explained by the inclusion of an empty 4p-orbital of Ga into the channel of ferromagnetic superexchange.[8a] In our case the nature of the metal does not change; therefore, the variation of the exchange type is caused by the interactions with apical ligand.

The comparison of the coordination site geometries of the complexes (Figure 7) and spin density distribution did not allow elucidation of the reason for the observable differences in the magnetic behavior of complexes **1**, **2**, and **3**−**7**. Single-point calculation of the model complex derived from complex **2** by the substitution of the apical methyl group by the halogen atom predicts the energy preference of the BS state with respect to the high spin one, i.e., the change of the character of the exchange interactions from ferro- to antiferromagnetic. Similarly, the replacement of the chlorine atom by a methyl group in complex **4** results in the ferromagnetic coupling in the model structure. Therefore, the character of the exchange in a series of the examined complexes is mostly determined by the orbital interactions conditioned by the nature of the apical atoms, and not by the stereochemistry of the coordination site, as it occurs in binuclear transition metal complexes.[31] Analysis of the singly occupied molecular orbitals ($\alpha + \beta$) of complex **2** shows (Figure 8a) that their shape on the semiquinonate ligands is analogous to that found for the magnetic orbitals of transition metal complexes.[29,30] The small contribution of gallium p-orbitals to SOMO ($\alpha + \beta$) promotes ferromagnetic exchange between remote semiquinone orbitals of complex **2**. The substitution of an alkyl group by a chlorine anion (complex **4**), accompanied by the change of the character of exchange interactions to antiferromagnetic, does not lead to alteration of the shape of the examined magnetic orbital. Therefore, the SOMO ($\alpha + \beta$) orbital is not responsible for the change in the character of exchange interactions in a series of the studied complexes. To explain the observed phenomenon, the other magnetic orbitals of complexes **2** and **4** have been considered. In complex **2**, there are two orbitals (SOMO − 9 and SOMO − 10) that can provide a channel of the magnetic exchange (Figure 8a). One of the magnetic orbitals of complex **4** (SOMO −11) is identical to SOMO − 10 of complex **2**; consequently, these orbitals do not cause the difference in the magnetic properties of the complexes concerned. Analysis of the orbitals SOMO − 9 of complex **2** and SOMO − 12 of complex **4** indicates that π orbitals of the oxygen and nitrogen atoms are taking part in their forming, but in the SOMO − 12 there is a contribution of the π orbital of the chlorine atom (Figure 8b), which results in the appearance of the antiferromagnetic exchange channel in complex **4** and in other compounds with inorganic anions (**3**, **5**−**7**).

The results of calculations of the exchange coupling parameters show good agreement with the experimental values; the deviations do not exceed 30 cm^{-1} which is in the range of the error of the method.[32] The exception is complex **7**, in which the difference reaches 60 cm^{-1}. To determine the cause of such a significant deviation, the comparison of the experimental and calculated geometries has been performed. It appeared that the largest differences occur in the structure of the apical NCS ligand. According to the X-ray data, the average distance N−C is 1.144 Å, and angle Ga−N−C is 168°, the analogous values found during the optimization of geometry are 1.188 Å and 180° correspondingly. It can be supposed that ascertained differences lead to the divergence of J values. With the aim to check this hypothesis the calculation of the exchange coupling parameter in the X-ray geometry has been performed, which results in the complete coincidence of the calculated value of J and the experimental data (Table 2). This finding is explained by the fact that the true geometry caused by the effect of the packing of the molecules in the crystal should be taken into account.

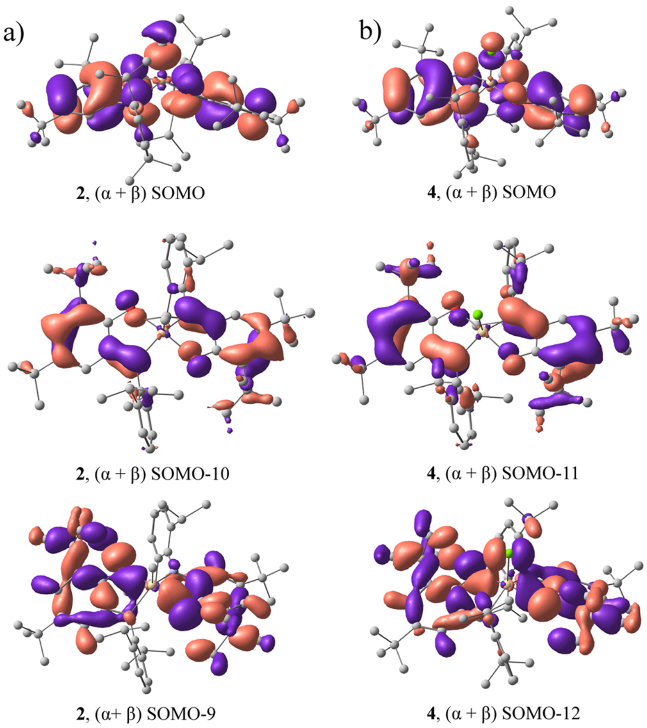

Figure 8. (a) Magnetic orbitals of the complex **2**. (b) Magnetic orbitals of the complex **4**.

■ CONCLUSION

The study of a series of pentacoordinated gallium bis-*o*-iminosemiquinonato complexes containing various auxiliary ligands (Et (**1**), Me (**2**), N_3 (**3**), Cl (**4**), Br (**5**), I (**6**), NCS (**7**)) has shown the strong dependence of the exchange coupling between spins of radical−anion ligands on the nature of the apical group. Magnetochemical investigations and quantum chemical analysis (UB3LYP/6-31G(d,p)) of magnetic orbitals provided an explanation of the unusual effect. The nature of the exchange interaction between the unpaired electrons of the iSQ ligands was found to be extremely sensitive to the nature of the apical group in the gallium coordination sphere. It was shown that the weak ferromagnetic coupling through the gallium orbitals is realized for complexes with the Et (**1**) and Me (**2**) apical groups. Another exchange pathway appears in complexes with N_3 (**3**), Cl (**4**), Br (**5**), I (**6**), and NCS (**7**) apical group. By means of quantum chemical calculations it has been shown that antiferromagnetic properties of the complexes with inorganic counterions are caused by the exchange channel including π orbitals of donor atoms. The value of magnetic exchange interactions varies from −99 (−68.6) to −176 (121.7) K (cm^{-1}) for R = I and R = NCS, respectively.

■ ASSOCIATED CONTENT

Ⓢ Supporting Information

EI mass spectrometric data, elemental analysis data, EPR spectra, molar magnetic susceptibility vs temperature data, and computational details for **1**−**7**. Crystallographic data in CIF format. The Supporting Information is available free of charge on the ACS Publications website at DOI: 10.1021/acs.inorgchem.5b00520.

■ AUTHOR INFORMATION

Corresponding Author

*E-mail: pial@iomc.ras.ru.

Notes

The authors declare no competing financial interest.

■ ACKNOWLEDGMENTS

This work was supported by the Russian Scientific Foundation (Grant 14-03-01296).

■ REFERENCES

(1) (a) Ovcharenko, V. I.; Sagdeev, R. Z. *Russ. Chem. Rev.* **1999**, *68*, 345−363. (b) Koivisto, B. D.; Hicks, R. G. *Coord. Chem. Rev.* **2005**, *249*, 2612−2630. (c) Vostrikova, K. E. *Coord. Chem. Rev.* **2008**, *252*, 1409−1419. (d) Ratera, I.; Veciana, J. *Chem. Soc. Rev.* **2012**, *41*, 303−349. (e) Iwamura, H. *Polyhedron* **2013**, *66*, 3−14. (f) Halcrow, M. A. *Spin-Crossover Materials, Properties and Applications*; John Wiley & Sons, Ltd.: New York, 2013. (g) Tezgerevska, T.; Alley, K. G.; Boskovic, C. *Coord. Chem. Rev.* **2014**, *268*, 23−40. (h) Faust, T. B.; D'Alessandro, D. M. *RSC Adv.* **2014**, *4*, 17498−17512.

(2) (a) Poddel'sky, A. I.; Cherkasov, V. K.; Abakumov, G. A. *Coord. Chem. Rev.* **2009**, *253*, 291−324. (b) Pierpont, C. G. *Coord. Chem. Rev.* **2001**, *219*−*221*, 415−433. (c) Pierpont, C. G. *Coord. Chem. Rev.* **2001**, *216*−*217*, 99−125.

(3) Loughrey, J. J.; Sproules, S.; McInnes, E. J. L.; Hardie, M. J.; Halcrow, M. A. *Chem.—Eur. J.* **2014**, *20*, 6272−6276.

(4) (a) Shultz, D. A.; Bodnar, S. H.; Vostrikova, K. E.; Kampf, J. W. *Inorg. Chem.* **2000**, *39*, 6091−6093. (b) Shultz, D. A.; Bodnar, S. H.; Lee, H.; Kampf, J. W.; Incarvito, Ch.D.; Rheingold, A. L. *J. Am. Chem. Soc.* **2002**, *124*, 10054−10061. (c) Shultz, D. A.; Vostrikova, K. E.; Bodnar, S. H.; Koo, H.; Whangbo, M.; Kirk, M. L.; Depperman, E. C.; Kampf, J. W. *J. Am. Chem. Soc.* **2003**, *125*, 1607−1617.

(5) (a) Cloke, F. G. N.; Hanson, G. R.; Henderson, M. J.; Hitchcock, P. B.; Raston, C. L. *J. Chem. Soc., Chem. Commun.* **1989**, 1002−1003. (b) Kaim, W.; Matheis, W. *J. Chem. Soc., Chem. Commun.* **1991**, 597−598. (c) Pott, T.; Jutzi, P.; Kaim, W.; Schoeller, W. W.; Neumann, B.; Stammler, A.; Stammler, H. G.; Wanner, M. *Organometallics* **2002**, *21*, 3169−3172. (d) Pott, T.; Jutzi, P.; Neumann, B.; Stammler, H. G. *Organometallics* **2001**, *20*, 1965−1967. (e) Baker, R. J.; Jones, C. *Dalton Trans.* **2005**, 1341−1348. (f) Schoeller, W. W.; Grigoleit, S. *J. Chem. Soc., Dalton Trans.* **2002**, 405−409. (g) Tuononen, H. M.; Armstrong, A. F. *Inorg. Chem.* **2005**, *44*, 8277−8284. (h) Tuononen, H. M.; Armstrong, A. F. *Dalton Trans.* **2006**, 1885−1894. (i) Antcliff, K. L.; Baker, R. J.; Jones, C.; Murphy, D. M.; Rose, R. P. *Inorg. Chem.* **2005**, *44*, 2098−2105. (j) Fedushkin, I. L.; Skatova, A. A.; Dodonov, V. A.; Chudakova, V. A.; Bazyakina, N. L.; Piskunov, A. V.; Demeschko, S.; Fukin, G. K. *Inorg. Chem.* **2014**, *53*, 5159−5170. (k) Fedushkin, I. L.; Sokolov, V. G.; Piskunov, A. V.; Makarov, V. M.; Baranov, E. V.; Abakumov, G. A. *Chem. Commun.* **2014**, *50*, 10108−10111.

(6) Chaudhuri, P.; Wagner, R.; Pieper, U.; Biswas, B.; Weyhermüller, T. *Dalton Trans.* **2008**, 1286−1288.

(7) (a) Lado, A. V.; Poddel'sky, A. I.; Piskunov, A. V.; Fukin, G. K.; Baranov, E. V.; Ikorskii, V. N.; Cherkasov, V. K.; Abakumov, G. A. *Inorg. Chim. Acta* **2005**, *358*, 4443−4450. (b) Piskunov, A. V.; Mescheryakova, I. N.; Fukin, G. K.; Bogomyakov, A. S.; Romanenko, G. V.; Cherkasov, V. K.; Abakumov, G. A. *Heteroat. Chem.* **2009**, *20*, 332−340. (c) Romanenko, G. V.; Ivakhnenko, E. P.; Minkin, V. I.; Starikov, A. G.; Bogomyakov, A. S.; Veber, S. L. *Inorg. Chim. Acta* **2014**, *418*, 66−72.

(8) (a) Ozarowsky, A.; McGarvey, B. R.; El-Hadad, A. A.; Tian, Z.; Tuck, D. G.; Krovich, D. J.; DeFotis, G. C. *Inorg. Chem.* **1993**, *32*, 841−847. (b) Adams, D. M.; Reingold, A. L.; Dei, A.; Hendrickson, D. N. *Angew. Chem., Int. Ed.* **1993**, *32*, 391−392. (c) Lange, C. W.; Conclin, B. J.; Pierpont, C. G. *Inorg. Chem.* **1994**, *33*, 1276−1283. (d) Piskunov, A. V.; Maleeva, A. V.; Fukin, G. K.; Bogomyakov, A. S.; Cherkasov, V. K.; Abakumov, G. A. *Dalton Trans.* **2011**, *40*, 718−725. (e) Piskunov, A. V.; Meshcheryakova, I. N.; Maleeva, A. V.; Bogomyakov, A. S.; Fukin, G. K.; Cherkasov, V. K.; Abakumov, G. A. *Eur. J. Inorg. Chem.* **2014**, 3252−3258.

(9) (a) Whalen, A. M.; Bhattacharya, S.; Pierpont, C. G. *Inorg. Chem.* **1994**, *33*, 347−353. (b) Chun, H.; Weyhermüller, T.; Bill, E.; Wieghardt, K. *Angew. Chem., Int. Ed.* **2001**, *40*, 2489−2492. (c) Chun, H.; Bill, E.; Weyhermüller, T.; Wieghardt, K. *Inorg. Chem.* **2003**, *42*, 5612−5620. (d) Herebian, D.; Ghosh, P.; Chun, H.; Bothe, E.; Weyhermüller, T.; Wieghardt, K. *Eur. J. Inorg. Chem.* **2002**, 1957−1967. (e) Poddel'sky, A. I.; Cherkasov, V. K.; Fukin, G. K.; Bubnov, M. P.; Abakumova, L. G.; Abakumov, G. A. *Inorg. Chim. Acta* **2004**, *357*, 3632−3640. (f) Bill, E.; Bothe, E.; Chaudhuri, P.; Chlopek, K.; Herebian, D.; Kokatam, S.; Ray, K.; Weyhermüller, Th.; Neese, F.; Wieghardt, K. *Chem.—Eur. J.* **2005**, *11*, 204−224. (g) Abakumov, G. A.; Cherkasov, V. K.; Bubnov, M. P.; Abakumova, L. G.; Ikorskii, V. N.; Romanenko, G. V.; Poddel'sky. *Russ. Chem. Bull.* **2006**, *55*, 44−52. (h) Smith, A. L.; Hardcastle, K. I.; Soper, J. D. *J. Am. Chem. Soc.* **2010**, *132*, 14358−14360. (i) Smith, A. L.; Clapp, L. A.; Hardcastle, K. I.; Soper, J. D. *Polyhedron* **2010**, *29*, 164−169.

(10) (a) Piskunov, A. V.; Meshcheryakova, I. N.; Ershova, I. V.; Bogomyakov, A. S.; Cherkasov, A. V.; Fukin, G. K. *RSC Adv.* **2014**, *4*, 42494−42505. (b) Piskunov, A. V.; Mescheryakova, I. N.; Bogomyakov, A. S.; Romanenko, G. V.; Cherkasov, V. K.; Abakumov, G. A. *Inorg. Chem. Commun.* **2009**, *12*, 1067−1070.

(11) Perrin, D. D.; Armarego, W. L. F.; Perrin, D. R. *Purification of Laboratory Chemicals*; Pergamon Press: Oxford, 1980.

(12) Piskunov, A. V.; Mescheryakova, I. N.; Ershova, I. V.; Fukin, G. K. *Inorg. Chem. Commun.* **2012**, *24*, 227−230.

(13) Piskunov, A. V.; Ershova, I. V.; Fukin, G. K. *Russ. Chem. Bull.* **2014**, *63*, 916−922.

(14) Gynane, M. J. S.; Wilkinson, M.; Worrall, I. J. *Inorg. Nucl. Chem. Lett.* **1973**, *9*, 765−766.

(15) *APEX2 v. 2013.20, Bruker Molecular Analysis Research Tool*; Bruker AXS: Madison, WI, 2013.

(16) Sheldrick, G.M. *SHELXTL v.6.12, Structure Determination Software Suite*; Bruker AXS: Madison, WI, 2000.

(17) Agilent Technologies. *CrysAlis Pro*; Agilent Technologies Ltd.: Yarnton, U.K., 2011.

(18) Frisch, M. J.; Trucks, G. W.; Schlegel, H. B.; Scuseria, G. E.; Robb, M. A.; Cheeseman, J. R.; Montgomery, J. A., Jr.; Vreven, T.; Kudin, K. N.; Burant, J. C.; Millam, J. M.; Iyengar, S. S.; Tomasi, J.; Barone, V.; Mennucci, B.; Cossi, M.; Scalmani, G.; Rega, N.; Petersson, G. A.; Nakatsuji, H.; Hada, M.; Ehara, M.; Toyota, K.; Fukuda, R.; Hasegawa, J.; Ishida, M.; Nakajima, T.; Honda, Y.; Kitao, O.; Nakai, H.; Klene, M.; Li, X.; Knox, J. E.; Hratchian, H. P.; Cross, J. B.; Bakken, V.; Adamo, C.; Jaramillo, J.; Gomperts, R.; Stratmann, R. E.; Yazyev, O.; Austin, A. J.; Cammi, R.; Pomelli, C.; Ochterski, J. W.; Ayala, P. Y.; Morokuma, K.; Voth, G. A.; Salvador, P.; Dannenberg, J. J.; Zakrzewski, V. G.; Dapprich, S.; Daniels, A. D.; Strain, M. C.; Farkas, O.; Malick, D. K.; Rabuck, A. D.; Raghavachari, K.; Foresman,

J. B.; Ortiz, J. V.; Cui, Q.; Baboul, A. G.; Clifford, S.; Cioslowski, J.; Stefanov, B. B.; Liu, G.; Liashenko, A.; Piskorz, P.; Komaromi, I.;Martin, R. L.; Fox, D. J.; Keith, T.; Al-Laham, M. A.; Peng, C. Y.; Nanayakkara, A.; Challacombe, M.; Gill, P. M. W.; Johnson, B.; Chen, W.; Wong, M. W.; Gonzalez, C.; Pople, J. A. *Gaussian 03, Revision E.01*; Gaussian, Inc.: Wallingford, CT, 2004.

(19) Becke, A. D. *J. Chem. Phys.* **1993**, *98*, 5648−5652.

(20) (a) Noodleman, L. J. *Chem. Phys.* **1981**, *74*, 5737−5743. (b) Yamaguchi, K.; Takahara, Y.; Fueno, T.; Nasu, K. *Jpn. J. Appl. Phys.* **1987**, *26*, L1362−L1364. (c) Yamaguchi, K.; Okumura, M.; Mori, W.; Maki, J.; Takada, K.; Noro, T.; Tanaka, K. *Chem. Phys. Lett.* **1993**, *210*, 201−210.

(21) Nakamoto, K. *Infrared and Raman Spectra of Inorganic and Coordination Compounds, Part B*, 5th ed.; Wiley: New York, 1997.

(22) Addison, A. W.; Rao, T. N.; Reedijk, J.; van Rijn, J.; Verschoor, G. C. *J. Chem. Soc., Dalton Trans.* **1984**, 1349−1356.

(23) Brown, S. N. *Inorg. Chem.* **2012**, *51*, 1251−1260.

(24) Cordero, B.; Gomez, V.; Platero-Prats, A. E.; Reves, M.; Echeverrıa, J.; Cremades, E.; Barragan, F.; Alvarez, S. *Dalton Trans.* **2008**, 2832−2838.

(25) Wertz, J. E.; Bolton, J. R. *Electron Spin Resonance. Elementary Theory and Practical Applications*; McGraw-Hill Book Company: New York, 1972.

(26) (a) Panthou, F. L.; Luneau, D.; Musin, R.; Öhrström, L.; Grand, A.; Turek, P.; Rey, P. *Inorg. Chem.* **1996**, *35*, 3484−3491. (b) Hostettler, M.; Törnroos, K. W.; Chernyshov, D.; Vangdal, B.; Bürgi, H.-B. *Angew. Chem., Int. Ed.* **2004**, *43*, 4589−4594. (c) Ovcharenko, V. I.; Romanenko, G. V.; Maryunina, K. Yu.; Bogomyakov, A. S.; Gorelik, E. V. *Inorg. Chem.* **2008**, *47*, 9537−9552. (d) Romanenko, G. V.; Maryunina, K. Yu.; Bogomyakov, A. S.; Sagdeev, R. Z.; Ovcharenko, V. I. *Inorg. Chem.* **2011**, *50*, 6597−6609.

(27) (a) Ovcharenko, V. I.; Gorelik, E. V.; Fokin, S. V.; Romanenko, G. V.; Ikorskii, V. N.; Krashilina, A. V.; Cherkasov, V. K.; Abakumov, G. A. *J. Am. Chem. Soc.* **2007**, *129*, 10512−10521. (b) Alley, K. G.; Poneti, G.; Robinson, P. S. D.; Nafady, A.; Moubaraki, B.; Aitken, J. B.; Drew, S. C.; Ritchie, C.; Abrahams, B. F.; Hocking, R. K.; Murray, K. S.; Bond, A. M.; Harris, H. H.; Sorace, L.; Boskovic, C. *J. Am. Chem. Soc.* **2013**, *135*, 8304−8323.

(28) (a) Speier, G.; Whalen, A. M.; Csihony, J.; Pierpont, C. G. *Inorg. Chem.* **1995**, *34*, 1355−1360. (b) Ivakhnenko, E. P.; Starikov, A. G.; Lyssenko, K. A.; Ovcharenko, V. I.; Bogomyakov, A. S.; Veber, S. L.; Minkin, V. I. *Inorg. Chim. Acta* **2014**, *410*, 144−149.

(29) Pierpont, C. G.; Attia, A. S. *Collect. Czech. Chem. Commun.* **2001**, *66*, 33−51.

(30) (a) Bachler, V.; Olbrich, G.; Neese, F.; Wieghardt, K. *Inorg. Chem.* **2002**, *41*, 4179−4193. (b) Herebian, D.; Wieghardt, K.; Neese, F. J. *Am. Chem. Soc.* **2003**, *125*, 10997−11005.

(31) Ruiz, E.; Alemany, P.; Alvarez, S.; Cano, J. *Inorg. Chem.* **1997**, *36*, 3683−3688.

(32) Ciofini, I.; Daul, C. A. *Coord. Chem. Rev.* **2003**, *238−239*, 187−209.

DOI: 10.1021/acs.inorgchem.5b00520
Inorg. Chem. 2015, 54, 6090−6099